

New coasts emerging from the retreat of Northern Hemisphere marine-terminating glaciers in the twenty-first century

Received: 24 March 2024

Accepted: 17 February 2025

Published online: 21 March 2025

 Check for updates

Jan Kavan ^{1,2}✉, Małgorzata Szczypińska ³✉, William Kochtitzky ⁴,
Louise Farquharson ⁵, Mette Bendixen ⁶ & Mateusz C. Strzelecki ³

Accelerated climate warming has caused the majority of marine-terminating glaciers in the Northern Hemisphere to retreat substantially during the twenty-first century. While glacier retreat and changes in mass balance are widely studied on a global scale, the impacts of deglaciation on adjacent coastal geomorphology are often overlooked and therefore poorly understood. Here we examine changes in proglacial zones of marine-terminating glaciers across the Northern Hemisphere to quantify the length of new coastline that has been exposed by glacial retreat between 2000 and 2020. We identified a total of $2,466 \pm 0.8$ km (123 km a^{-1}) of new coastline with most (66%) of the total length occurring in Greenland. These young paraglacial coastlines are highly dynamic, exhibiting high sediment fluxes and rapidly evolving landforms. Retreating glaciers and associated newly exposed coastline can have important impacts on local ecosystems and Arctic communities.

The Arctic has warmed up to four times faster than the rest of the globe during the last 40 years¹ and global temperatures are expected to warm further in the coming decades², which will lead to important glacier retreat during the twenty-first century³. Marine-terminating glaciers in the Northern Hemisphere have undergone a net mass loss due to terminus retreat of $10.3 \pm 3.4 \text{ Gt a}^{-1}$ in the period 2000–2020⁴. Ongoing climate change and associated glacier retreat result in the rapid proliferation of paraglacial coastlines⁵. More than 900 km of new coastline has been identified by remote sensing analysis in Svalbard alone since the 1930s⁶. Glacier dynamics have been studied widely at a global scale⁷, especially in association with sea-level rise⁸ and its consequences for terrestrial ecosystems⁹. However, little work has focused on determining the rate and extent of new paraglacial coastline formation despite the ecological importance of these regions as emergent habitats across extensive regions of the Arctic¹⁰.

As marine-terminating glaciers retreat they reveal new coasts that often consist of unconsolidated glacial landforms, such as moraines, eskers, crevasse squeeze ridges or glaciofluvial deposits and deltas, as well as glacially polished bedrock¹¹. In some cases, the newly exposed coastline is in the form of rocky islands^{12,13}. The paraglacial coast exposed from beneath glacial ice differs from much of the Arctic coast as it is not initially affected by permafrost, which needs 2 years or more to aggrade after deglaciation^{14,15}. This lack of permafrost and associated ice cementation means that sediment can be easily eroded, transported and deposited, creating an Arctic system that is geomorphologically uniquely dynamic. In addition to the regular coastal processes of erosion and reworking by ocean currents, tides and wind waves, these newly formed paraglacial coastlines are exposed to extreme waves. These often tsunami-like waves are triggered by deglaciation processes including (1) glacial calving¹⁶, (2) iceberg rolling¹⁷ and (3) landslides and rockfalls¹⁸.

¹Centre for Polar Ecology, University of South Bohemia, Branišovská, Czechia. ²Polar-Geo Lab, Department of Geography, Faculty of Science, Masaryk University, Brno, Czechia. ³Alfred Jahn Cold Regions Research Centre, Institute of Geography and Regional Development, University of Wrocław, Wrocław, Poland. ⁴School of Marine and Environmental Programs, University of New England, Biddeford, MA, USA. ⁵Geophysical Institute, University of Alaska Fairbanks, Fairbanks, AK, USA. ⁶Department of Geography, McGill University, Montreal, Quebec, Canada. ✉e-mail: jkavan@prf.jcu.cz; malgorzata.szczypinska2@uwr.edu.pl

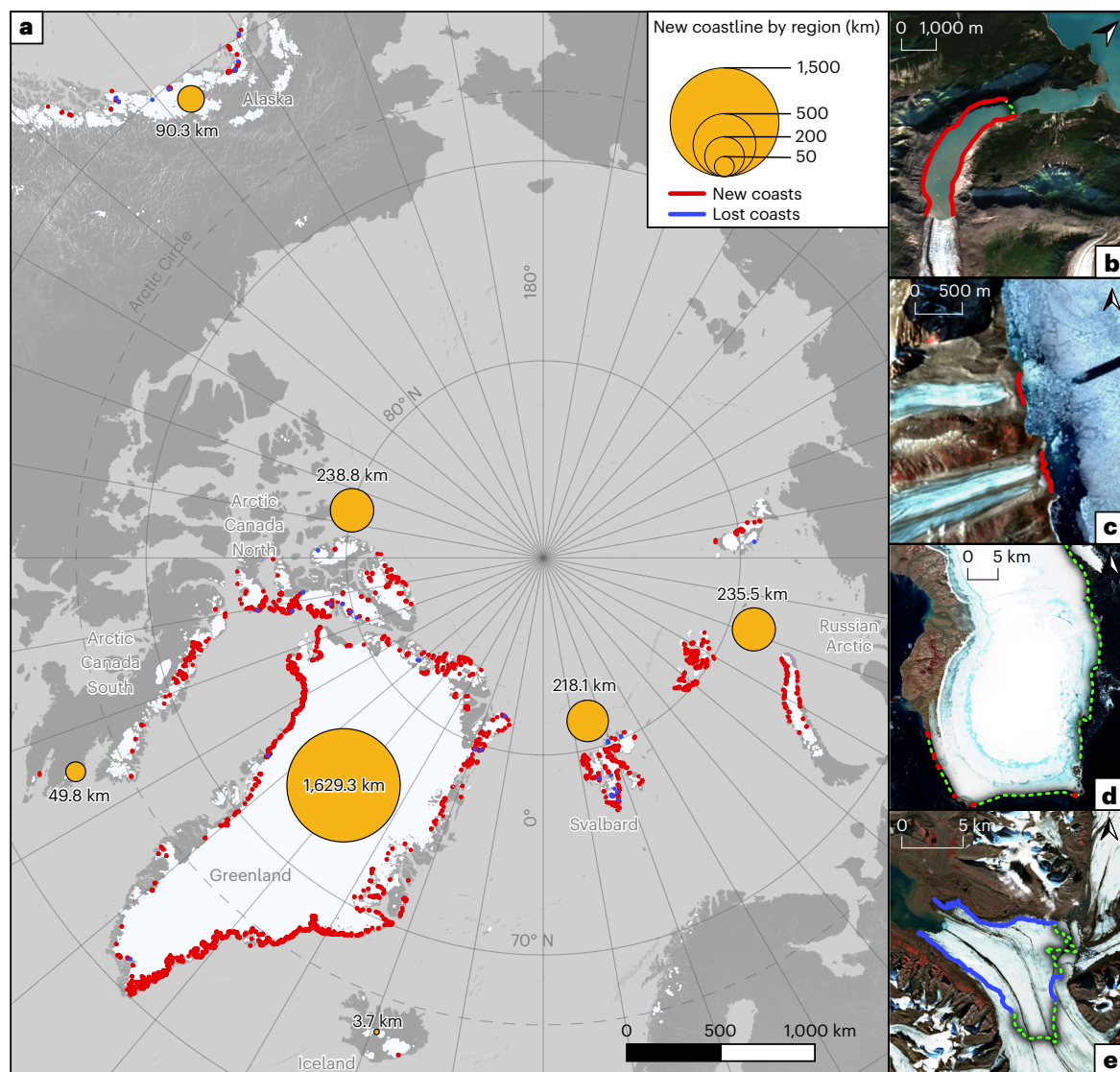


Fig. 1 | Spatial distribution and examples of new and lost coastlines in the Arctic from 2000 to 2020. Examples shown by photographs from 2020 with marked glaciers front positions in 2000 (green dotted lines). **a**, Spatial distribution of new (red) and lost (blue) coastline. Lost coastline displayed as the top layer in the map. **b**, Alaska example of Sawyer Glacier (Randolph Glacier Inventory identifier RGI60-01.20968) with relatively long new coastline due to narrow topography. **c**, Arctic Canada South example of the outlet glaciers on

Baffin Island (RGI60-04.03406 and RGI60-04.03405) which became land-terminating during the study period resulting in relatively long new exposed coastline (glacier fronts positions in 2000 are similar to the coastline position in 2020). **d**, Russian Arctic example of ice cap retreat with little coast change on Graham Bell Island (RGI60-09.00986). **e**, Nathorstbreen glacier (Svalbard, RGI60-07.00298) responsible for almost half the lost coastline of the Northern Hemisphere as a result of the major surge.

The retreat of marine-terminating glaciers not only alters the landscape but simultaneously poses an indirect risk to local communities and economic activities in the coastal zone. Regions around marine-terminating glaciers have an enhanced susceptibility to landslide-triggered tsunamis; for example, the one recorded on 17 June 2017 in Greenland, which caused substantial infrastructure damage and loss of life¹⁹. Calving fronts of tidewater glaciers, where small tsunamis frequently form are often visited by tourists for their beauty and abundant wildlife²⁰. Camping and touristic activities along coasts close to the main iceberg transport routes are threatened by iceberg roll waves (for example, ref. 21). Apart from health and safety risks linked to extreme wave impacts, the tourism industry may be considerably compromised by the scenic beauty of the landscape when marine-terminating glaciers morph into land-terminating features²². Conversely, the retreat of glaciers on land results in the termination of iceberg production, leading to safer sailing conditions. The recession of

glaciers can lead to increased sediment production (for example, delta formation) and easier access to sediment deposits, which in the case of Greenland, can promote the economic independence of the region²³.

Here we illustrate the impact of marine-terminating glacier retreat on the origin and development of new Arctic coasts in the twenty-first century. We use the dataset of Northern Hemisphere marine-terminating glacier retreat between 2000 and 2020²⁴ to identify all marine-terminating glaciers in the Northern Hemisphere and as a source of year 2000 glacier fronts positions. Using satellite imagery, we manually digitize the new coastline exposed as a result of glacier retreat and the coastline that has disappeared as a result of glacier advances. We identify ~2,500 km of new coastline released from glacial ice that formed across the Arctic since 2000, analyse it by region and characterize some of the environmental factors affecting coastal evolution, such as exposed rock type, occurrence of permafrost and recent climatic conditions.

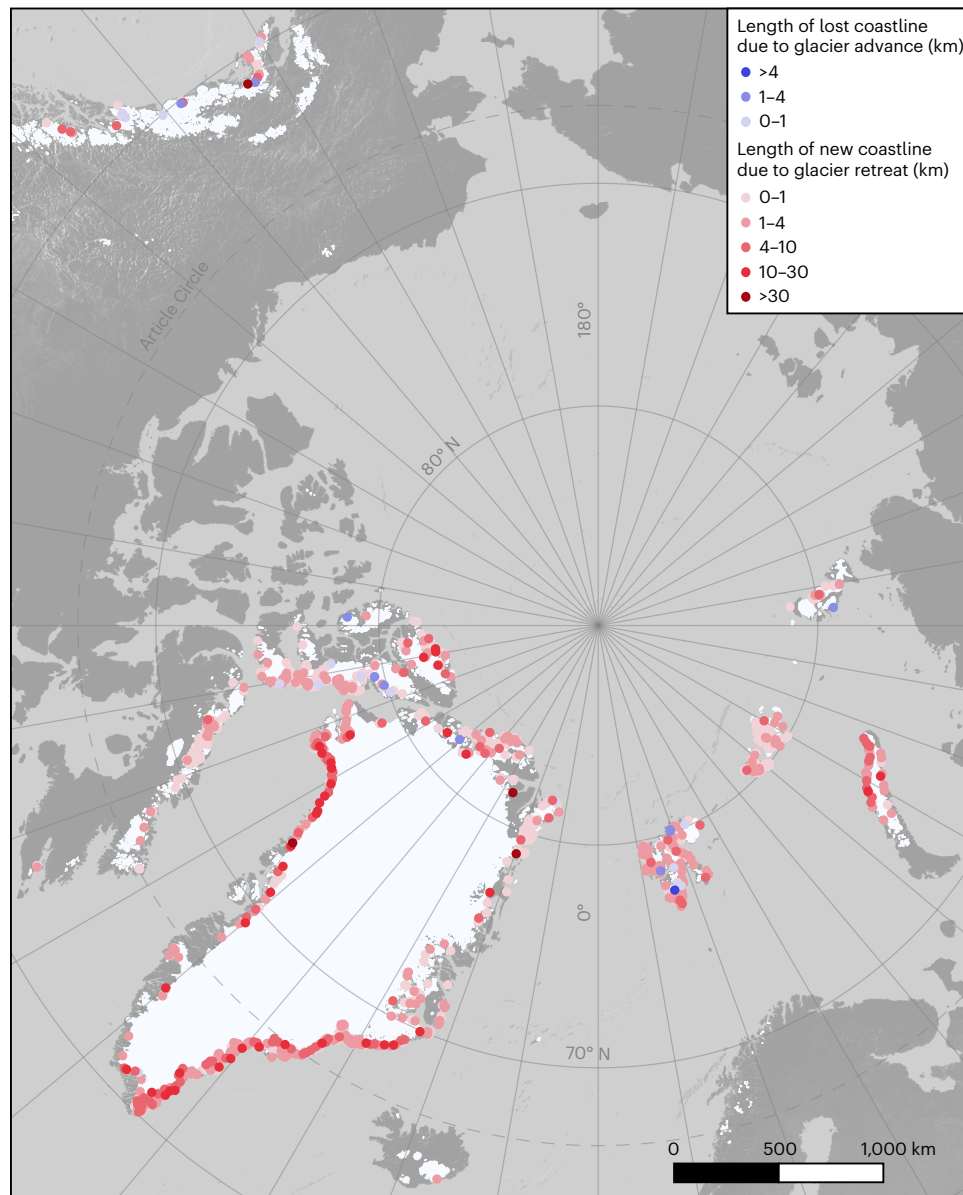


Fig. 2 | Length of new and lost coastlines marked by individual glaciers. Glaciers connected with the longest new and the longest lost coastline are displayed in the front.

New and lost coastlines of the Arctic

We analysed 3,217 sections of Northern Hemisphere coastline (Fig. 1) developing in front of marine-terminating glaciers to explore the rate of coastline formation due to glacier retreat. Our results show that $2,466 \pm 0.8$ km of new coastline has formed between 2000 and 2020 giving an average length of 123 km of new coast every year. Two-thirds (66%) of this coastline was exposed in Greenland—the largest region of the Arctic also with the highest glacier coverage. The Northern Canadian Arctic, Russian Arctic and Svalbard contributed similarly with 218–240 km of new coastline (9–10% each). The remaining part is divided among Alaska, Southern Canadian Arctic and Iceland (Fig. 1, Supplementary Table 1 and Supplementary Fig. 1). More than half of the total additional coastline length is derived from only 101 glaciers—6% of all marine-terminating glaciers in the Northern Hemisphere and 8% of the glaciers that uncovered any new coastline (Fig. 2).

The retreat of a glacier does not automatically lead to the origin of a new coast. Of the 1,704 marine-terminating glaciers reported by ref. 24, 1,453 (85%) retreated, and we find that 1,206 (71%) led to

the development of new coastline. The absence of new coastline despite glacial retreat was mainly the result of a small amount of retreat in the central part of the glacier terminus that did not affect its lateral margin zones or in the case of outlet glaciers or marine-based ice caps where there is no lateral contact with land. The last was frequently observed in the Russian Arctic (particularly Franz Joseph Land), where only 48% of marine-terminating glaciers developed new coastline. The other regions have a rather uniform ratio of glaciers with newly developed coastlines compared to the number of all marine-terminating glaciers (71–88%), except Iceland where only one marine-terminating glacier is present (Supplementary Table 1 and Supplementary Fig. 2).

Regions with the greatest reduction in glacier areal extent did not necessarily correlate with the areas of most coastline gain. After normalizing coastal gain by glacier area retreat, we found that, on the contrary to overall length of gained shoreline, it is not Greenland but Alaska and Arctic Canada South that are the most efficient regions in forming new coast (Fig. 3).

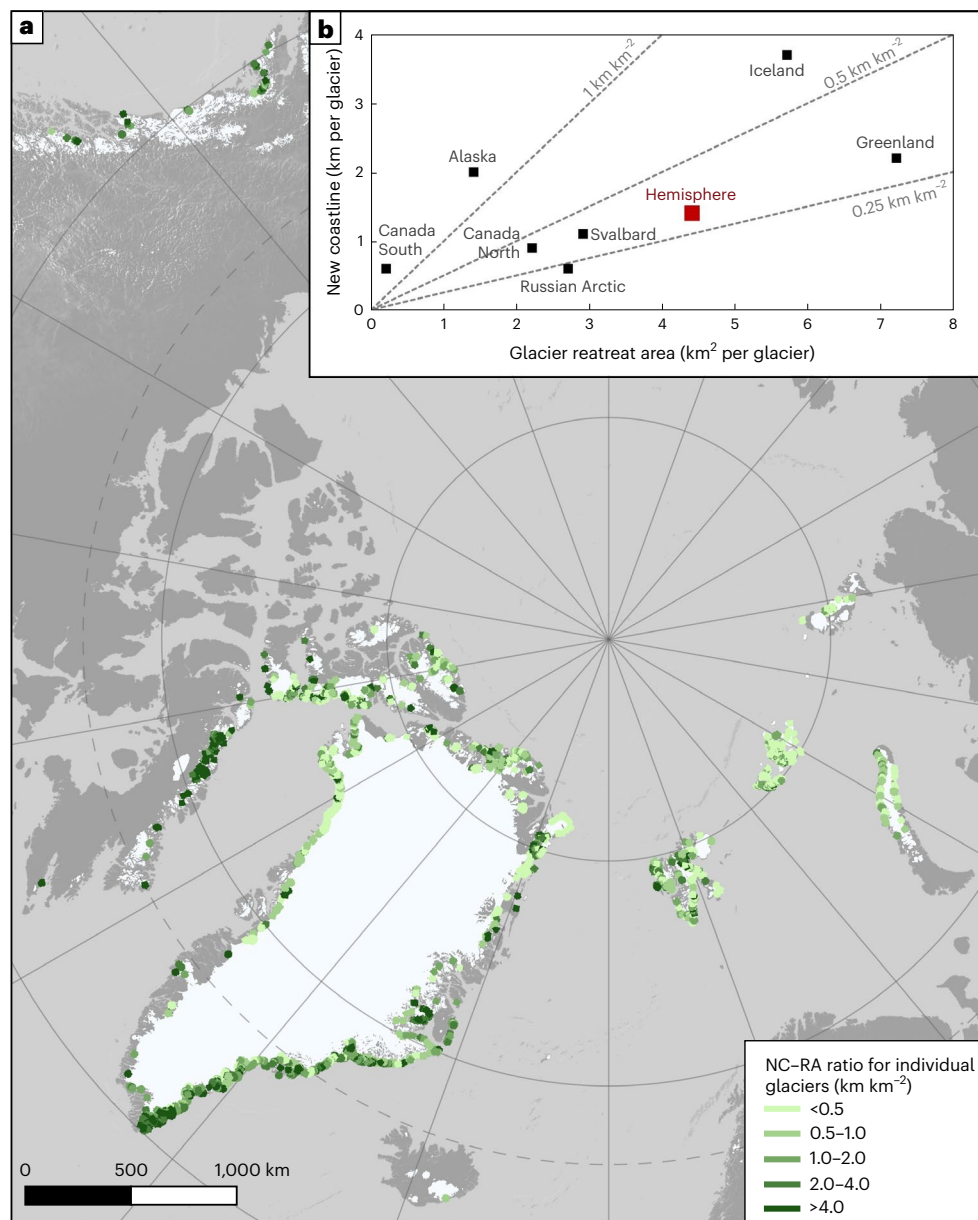


Fig. 3 | Comparison between new coastline length and retreat area for the period 2000–2020 for individual glaciers and for study regions. Data on glacier areal retreat adjusted from ref. 24. **a**, Map of NC-RA ratios for individual

glaciers. **b**, Regional differences in glacier areal retreat and resulting new coastline origin; all marine-terminating glaciers are included; red square represents hemisphere average.

In contrast to newly exposed coastline (2,466 km), we identified only 53.1 ± 0.1 km of coastline that was lost due to glacier advances, including surging. Most of this lost coastline is reported from Svalbard (63%), where a major surge of the Nathorstbreen glacier system buried nearly 26 km of coastline present in 2000. This single glacier therefore accounts for almost half of the lost coastline of the Northern Hemisphere (Fig. 1d). Length of lost coastline by regions can be found in Supplementary Table 1 and compared on Supplementary Fig. 1.

New islands

Retreating glaciers not only expose new coasts but also uncover new islands. We identified 35 new islands larger than 0.5 km^2 that were completely uncovered or lost their glacial connection with the mainland during the period 2000–2020. Most ($n = 29$) new islands are in Greenland with only six in Svalbard and the Russian Arctic. Here we report 13 new islands: 12 that separated from Greenland and 1 that separated from Severnaya Zemlya in the Russian Arctic. However, five of those

islands (with four related to the same glacier) are already on maps from the 1960s, suggesting substantial advance of these two glaciers in the late twentieth century (islands 12 (ref. 25) and 14–17 (ref. 26)). Glacial advance resulted in ice covering the islands in the late twentieth century and glacial retreat during the last two decades has led to their reappearance. Spatial distribution and examples of new islands are shown in Fig. 4 and more data concerning specific islands can be found in Supplementary Table 2.

Environmental conditions along newly emerged coasts

To evaluate the efficiency of the coastal processes operating along deglaciated terrains we compiled key information regarding the dominant geology, permafrost coverage and climate (mean annual temperature (MAT) and precipitation in period 2000–2020) (Fig. 5).

The geological description was generalized to categories of sedimentary, igneous, metamorphic and undivided rocks based on ref. 27.

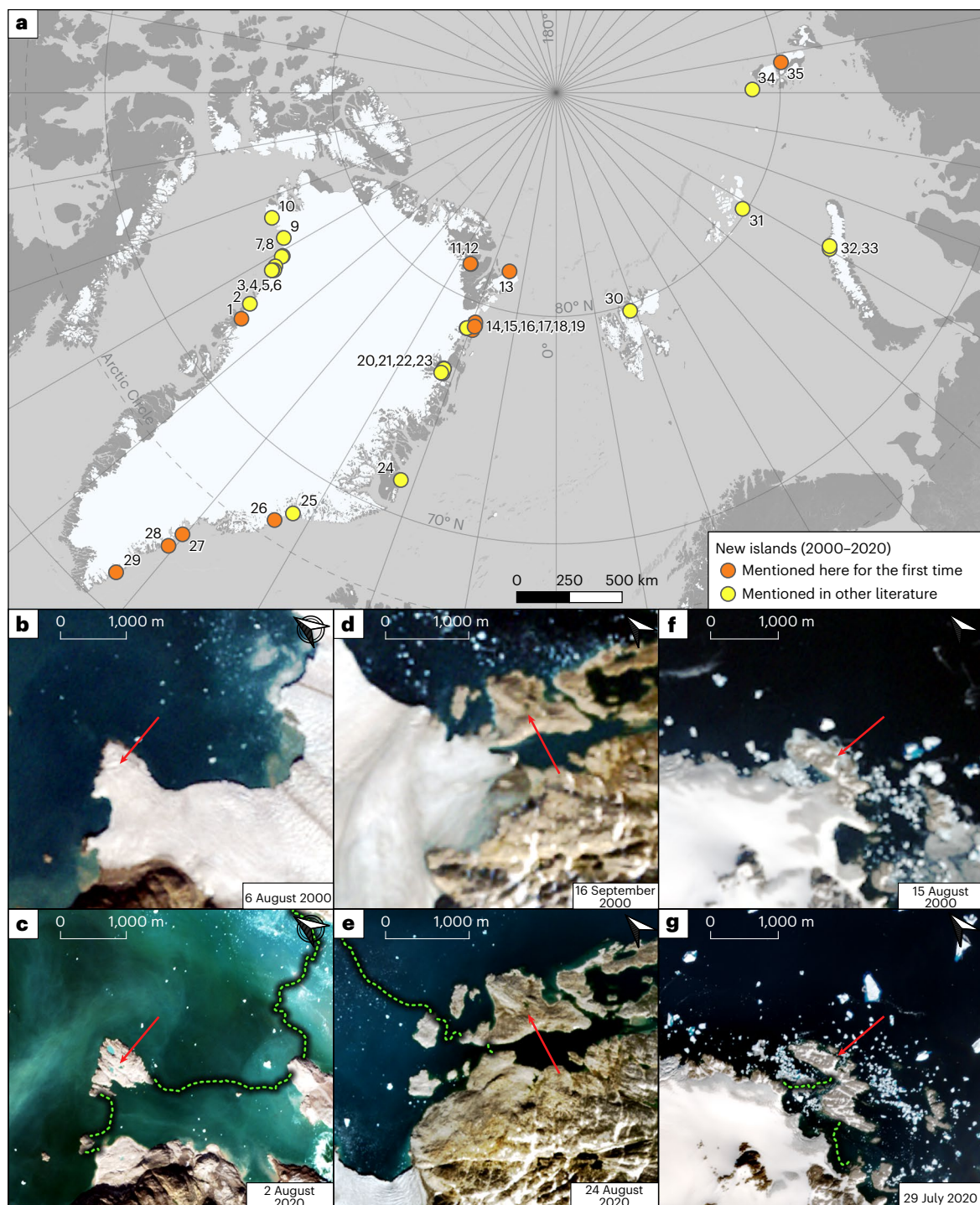


Fig. 4 | Map and examples of new islands detected from the period 2000–2020 in the Arctic. a–g. Map of new islands (a); island no. 1 (b in 2000, c in 2020); island no. 29 (d in 2000, e in 2020); and island no. 27 (f in 2000, g in 2020). Green line marks the year 2000 glacier front position and the red arrow marks the island of interest.

The majority of new coastline is formed in areas of metamorphic bedrock (Fig. 5). Sedimentary rocks, which are generally softer and more susceptible to erosion^{28,29}, dominate along the eastern coasts of Svalbard (Fig. 5). Small stretches of coastline made up of sedimentary rocks have also been exposed in the Arctic regions of Canada, Alaska and the northern fringes of Greenland.

New coastlines are forming across a range of permafrost zones from continuous (underlying 90–100% of the landscape) to isolated (underlying 10% or less of the landscape). In northern continuous permafrost regions, the mean annual ground temperature at the depth

of zero amplitude ranges from -5 to -10 °C (ref. 30), with some of the coldest sites exhibiting a mean annual ground temperature down to -15 °C (for example, Alert, Canada, 82° N at 15 m depth³⁰). More than half of new coasts detected in our study were found in this zone (Fig. 2). The most southerly new coastal sites mapped (Alaska, Iceland and southeastern Greenland) are in the sporadic to isolated permafrost zone where the mean annual ground temperature at the depth of zero amplitude is close to freezing at >-1 °C.

The climatic indices are highly variable, with average air temperature spanning from $+6$ to -20 °C and precipitation from <100 to

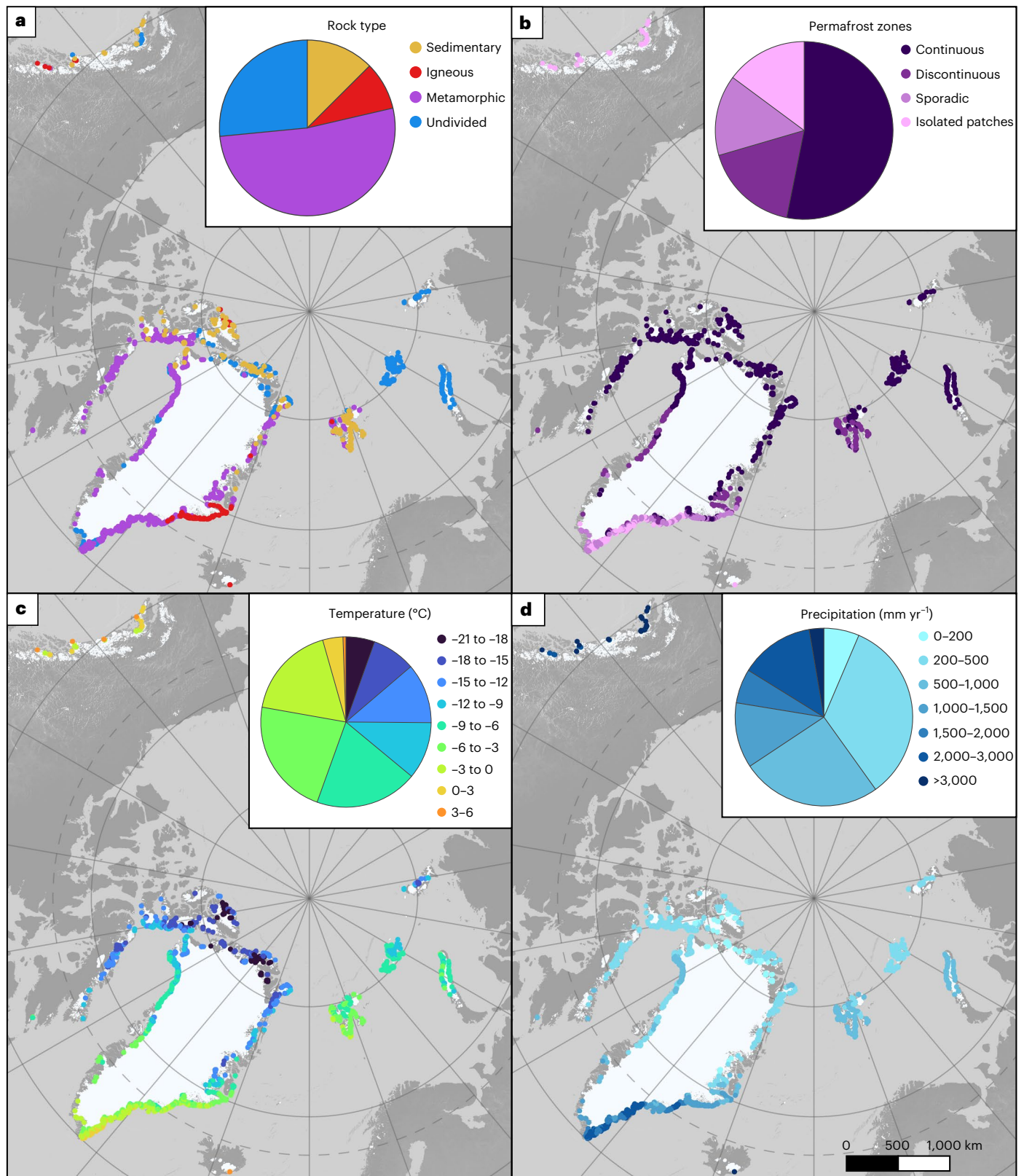


Fig. 5 | Geological and climatic summaries of newly emerged coastlines. a–d, General rock types (a), permafrost zones (b), MATs (mean for period 2000–2020) (c) and annual precipitation (mean for period 2000–2020) (d). Diagrams refer

to the total length of new coastline segments attributed to the particular class. Data sources: rock type, ref. 27; permafrost zones, ref. 65; and temperature and precipitation ERA5 data, ref. 66.

>4,000 mm in the region (Fig. 5). More than a quarter of new coastline length is characterized by MAT below -12°C and more a half by MAT below -7°C . Only 4% (nearly 110 km) occurs in places with positive

MAT, where frost cracking, potentially leading to further rock surface weathering, is expected to be more efficient³¹. All these sections, present in Alaska, Iceland and southeast Greenland, are at the same

time very humid with precipitation exceeding 1,800 mm, which may facilitate substantial sediment mobilization by fluvial processes. MAT and annual precipitation in the areas of new coasts can be found in Supplementary Table 3.

Discussion

The major factor controlling paraglacial coastline lengthening in the northern hemisphere is the retreat of marine-terminating glaciers. The most dramatic retreat and new coast emergence were formed as a result of the collapse of either ice shelves or the floating portion of a marine-terminating glacier (floating glacier tongue)²⁴. Disintegration of ice shelves derived from floating glacier tongues and multidecadal fast sea ice is characteristic for the northernmost part of Greenland³² and Canada (Ellesmere Island³³), where most of the glaciers retreated between 1999 and 2015 to their grounding lines and lost connection with the sea³⁴. According to ref. 24, three other factors promoting substantial retreat are: (1) if the glacier surges, (2) if the glacier has variable bed topography or (3) if the glacier has substantially wide calving margins (see also refs. 35,36).

Recent marine-terminating glacier retreat is usually controlled by increasing ocean temperature^{37–39} or a combination of ocean and atmosphere warming⁴⁰. Other controlling factors that lead to high spatial and temporal variability of the retreat rate include the location of pinning points, other topographic characteristics (configuration of the coastline) and variations in snowfall distribution⁴¹. Glacier retreat may be influenced by increasing frequency of extreme atmospheric events, such as atmospheric-river-induced foehn events. These events have spatially variable effect and can lead to high melt rates of some Greenlandic glaciers⁴² or glaciers in the Russian Arctic⁴³. Climate warming in the twenty-first century has serious consequences for marine-terminating glaciers for example in the Canadian Arctic Archipelago^{44,45}, Russian Arctic⁴⁶ or Atlantic Arctic⁴¹, where the retreat rate after 2000 is known to be markedly higher than during the twentieth century.

It is important to highlight that retreat rate as well as coastline exposure rate are not constant in time and minor advances are detected even among the fastest retreating glaciers³⁷. Some glaciers exhibit nonlinear behaviour through a mix of retreat and advance episodes whereby any coastline exposed in a retreat phase was later lost by advance (for example, Nathorstbreen glacier surge⁴⁷; Fig. 1d).

The extent of coastline emergence is tightly connected to local topography with more complex and elongate shapes (for example, narrow fjords) resulting in a higher new coastline to retreat area (NC–RA) ratio. Glaciers with termini that extended out into the open sea could experience extensive retreat without any new coastline formation. Coastal morphology is connected to long-term local climate, especially air temperature and precipitation rates that affect overall glacier mass balance and predispose glacier sliding (Supplementary Fig. 3 representing glacier velocity as a proxy for glacier sliding), affecting the erosion efficiency of the glacier^{48–50}. Spatially variable erosion rates can also be an effect of varying underlying geology⁵¹. Glacial valleys formed in softer rocks tend to be shallower and wider²⁹. Our analysis shows a strong relationship between NC–RA ratio and rock type category being either (1) sedimentary rocks (as generally being more easily erodible) or (2) igneous and metamorphic rocks. Sedimentary rocks proved to be connected to less effective coastline gain. However, at least part of this correlation should be attributed to specific spatial distribution of sedimentary rock units in the Arctic, especially in Greenland (Supplementary Analysis). Tectonic uplift, present among our study regions, mainly in Alaska and Iceland can also be an important driver of glacial erosion^{52,53} and therefore potentially important in the development of new soft coastlines.

Greenland contains the largest average glacier retreat area in the Arctic (Fig. 3). The glacier with the longest new coastline, Zachariae Isstrom in northeast Greenland, is responsible for >81 km of new coastline, which is more than twice as much as any other glacier in the hemisphere (dataset³⁴). The majority of glaciers exposing the longest

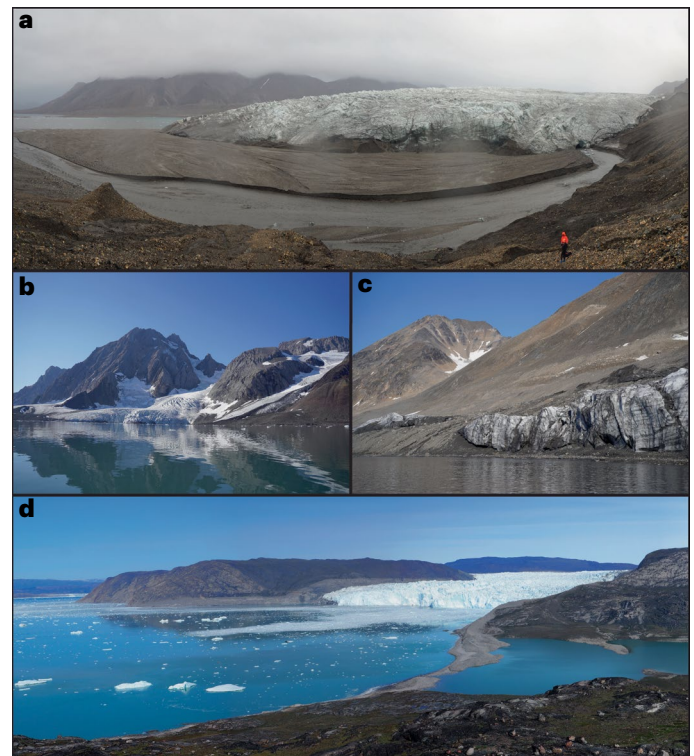


Fig. 6 | Geodiversity of new coastlines developed after retreat of Arctic marine-terminating glaciers. **a**, Young delta system accumulated in the lagoon exposed by Recherchebreen, Svalbard. **b**, Rocky cliffs and morainic cliffs released from retreating Samarinbreen, Svalbard. **c**, Juvenile beach system in Brepollen supplied by glacial sediment dropping from remnants of ice cliffs. **d**, Erosion of a lateral moraine by calving waves from Eqip Sermia, Western Greenland, leading to extension of the spit system along the southern coast. Credit: **b,c**, Aleksandra Osika.

coastline are in Greenland with almost all of them attached to the ice sheet. However, the low NC–RA ratio makes it second least effective among our study regions in producing new coastline compared to glacier areal retreat. This is generally due to the wide glacier tongues in the north of Greenland, that terminate in ice shelves³². Others⁵⁵ studied 199 marine-terminating glaciers in Greenland in the early 2000s, out of which only 11 showed overall advance and the total retreat was 267 km from 2000 to 2010. Our finding of 1,629 km of new coastline in Greenland seems to be of the same order of magnitude considering the timescale and typical shape of fjords (that is, two new coasts forming on either side of a fjord). However, our study includes all tongues of each glacier, while ref. 55 focus on the main trunks.

Examples from Alaska demonstrate the importance of topographic controls on the behaviour of the glaciers. Retreating glaciers in deep and narrow fjords expose long coastal zones with only minor areal change (Fig. 1a). While Alaska has the second lowest areal retreat rate, it exhibited one of the longest new coastlines with a high NC–RA ratio (Fig. 3). This can be explained by deep fjords that are formed as a result of high erosion rates resulting from high precipitation, relatively high temperatures (Fig. 5), as well as tectonic activity related to proximity to a convergent plate boundary. The effect of soft sedimentary bedrock present along numerous coastline sections (Fig. 5), which may contribute to valleys widening and therefore lower NC–RA ratios, seems to be negligible.

In contrast to our observations from Alaska, the configurations of glaciers in Franz Josef Land (Russian Arctic) are not favourable for exposing long coastlines. The archipelago differs from the rest of the Arctic in glaciation style (ice caps and ice shelves instead of grounded glaciers and ice streams channelized in steep and narrow fjords).

Glaciers here have low slopes and terminate in wide floating tongues surrounded by the open sea⁵⁶. Here even considerable retreat may lead only to the minor exposure of new coasts, if any (Fig. 1c).

Southern Arctic Canada stands out for its high NC–RA ratio. Despite the relatively short new coastline per glacier, the ratio is extremely high as a result of very little average area change. This region is characterized by small ice caps with numerous narrow glacier snouts. Narrow glacial valley morphology and extensive coastline emergence in the region can be partly explained by the bedrock as new shorelines are generally characterized by resistant metamorphic bedrock that erodes slowly (Fig. 5). More than half of the glacier tongues changed or nearly changed from marine-terminating to land-terminating during the period of 2000–2020 and therefore produced new coastlines not only perpendicular to ice flow but also parallel to the glacier front (Fig. 1b). This observation highlights the fact that small glaciers matter when considering the coastal dynamics and appearance of new coast.

Retreating, warm-based glaciers uncover the bedrock surface which can then be exposed to below-zero mean annual air temperatures. After 2 or more years, this may lead to permafrost aggradation that may take decades to reach equilibrium with the climate⁵⁷. In general, permafrost aggradation is expected to be limited to new coastlines in the continuous permafrost zone where mean annual air temperature is sufficiently low. Implications of permafrost aggradation vary, depending on lithology. Along sedimentary shorelines, permafrost aggradation could affect the rate of geomorphological change as it leads to the cementation of sediment with ice⁵⁸. Along bedrock shorelines, permafrost has a limited influence on coastal zone processes⁵⁹, although ice filling of rock joints can increase the strength of permafrost-affected fractured bedrock⁶⁰. Ongoing climate warming is expected to cause long-term permafrost thaw and ice warming consequently destabilizing adjacent slopes in coming decades and centuries, which will continue to influence the geomorphology of new coastlines.

Our analyses show that the majority of new coast is forming in relatively resistant bedrock, continuous permafrost zone and relatively harsh climatic conditions, which may prevent rapid coastal change (that is, erosion). For new coastlines forming in cold continuous permafrost, aggradation of new permafrost is likely to occur fairly rapidly (<5 years). The development of new permafrost in the discontinuous, sporadic and isolated zones is more challenging to predict because of the variable influence of lithology, topography and vegetation dynamics. Where permafrost does form, it can lead to ice cementation along sections of unlithified coastline, potentially making these new coastlines more resilient to erosion.

Coasts built in sedimentary strata are the most prone to fast sediment generation and redistribution⁶¹. These regions, such as eastern Svalbard, may be considered hotspots in terms of expected coastal dynamics. In regions characterized by an abundance of sediments released from retreating glaciers, such as Svalbard, Alaska and southern Greenland, rapid formation of accumulative landforms (such as deltas) is observed (for example, refs. 62,63).

An alternative process occurs when rapid glacial retreat exposes bedrock and may lead to changes in internal rock stress, increased erosion and weathering. This may lead to rapid slope deformations, such as rockfalls or landslides, triggering tsunamis in extreme cases as reported from sites around Alaska and Greenland (for example, ref. 64).

The observed formation of young paraglacial coastal environments emerging from the retreat of Northern Hemisphere marine-terminating glaciers (for examples, see Fig. 6) foreshadows coastal evolution in the ice-free Arctic of a warmer future. Both accumulative (beaches, deltas, barriers and tidal flats) and rocky (cliffs, stacks, skerries and shore platforms) coastal systems will rapidly adjust to non-glacial conditions on land and a decline in sea ice extent and duration. How quickly the sediments and landforms left along these shores lose their glacial characteristics and become a new coastal environment, no longer controlled by the presence of glacial ice, remains a knowledge gap.

Online content

Any methods, additional references, Nature Portfolio reporting summaries, source data, extended data, supplementary information, acknowledgements, peer review information; details of author contributions and competing interests; and statements of data and code availability are available at <https://doi.org/10.1038/s41558-025-02282-5>.

References

- Rantanen, M. et al. The Arctic has warmed nearly four times faster than the globe since 1979. *Commun. Earth Environ.* **3**, 168 (2022).
- Lee, J.-Y. et al. in *Climate Change 2021: The Physical Science Basis* (eds Masson-Delmotte, V. et al.) 553–672 (Cambridge Univ. Press, 2023).
- Rounce, D. R. et al. Global glacier change in the twenty-first century: every increase in temperature matters. *Science* **379**, 78–83 (2023).
- Kochtitzky, W. et al. The unquantified mass loss of Northern Hemisphere marine-terminating glaciers from 2000–2020. *Nat. Commun.* **13**, 5835 (2022).
- Irrgang, A. M. et al. Drivers, dynamics and impacts of changing Arctic coasts. *Nat. Rev. Earth Environ.* **3**, 39–54 (2022).
- Kavan, J. & Strzelecki, M. C. Glacier decay boosts the formation of new Arctic coastal environments—perspectives from Svalbard. *Land Degrad. Dev.* **34**, 3467–3474 (2023).
- Millan, R., Mouginit, J., Rabatel, A. & Morlighem, M. Ice velocity and thickness of the world's glaciers. *Nat. Geosci.* **15**, 124–129 (2022).
- Edwards, T. L. et al. Projected land ice contributions to twenty-first-century sea level rise. *Nature* **593**, 74–82 (2021).
- Ficetola, G. F. et al. The development of terrestrial ecosystems emerging after glacier retreat. *Nature* **632**, 336–342 (2024).
- Krause-Jensen, D. & Duarte, C. M. Expansion of vegetated coastal ecosystems in the future Arctic. *Front. Mar. Sci.* **1**, 77 (2014).
- Strzelecki, M. C. et al. New fjords, new coasts, new landscapes: the geomorphology of paraglacial coasts formed after recent glacier retreat in Brepollen (Hornsund, southern Svalbard). *Earth Surf. Process. Landf.* **45**, 1325–1334 (2020).
- Ziaja, W. & Ostafin, K. Origin and location of new Arctic islands and straits due to glacial recession. *Ambio* **48**, 25–34 (2019).
- Ziaja, W. & Haska, W. The newest Arctic islands and straits: origin and distribution, 1997–2021. *Land Degrad. Dev.* **34**, 1984–1990 (2023).
- Mackay J. R. A full-scale field experiment (1978–1995) on the growth of permafrost by means of lake drainage, western Arctic coast: a discussion of the method and some results. *Can. J. Earth Sci.* **34**, 17–33 (1997).
- Rangel, R. C. et al. Geophysical observations of taliks below drained lake basins on the Arctic coastal plain of Alaska. *J. Geophys. Res. Solid Earth* **126**, e2020JB020889 (2021).
- Kostrzewa, O. et al. A boulder beach formed by waves from a calving glacier revisited: multidecadal tsunami-controlled coastal changes in front of eqip sermia, west greenland. *Permafrost. Periglac. Process* **35**, 312–325 (2024).
- Wolper, J. et al. A glacier–ocean interaction model for tsunami genesis due to iceberg calving. *Commun. Earth Environ.* **2**, 130 (2021).
- Svennevig, K. et al. A rockslide-generated tsunami in a Greenland fjord rang Earth for 9 days. *Science* **385**, 1196–1205 (2024).
- Strzelecki, M. C. & Jaskólski, M. W. Arctic tsunamis threaten coastal landscapes and communities – survey of Karrat Isfjord 2017 tsunami effects in Nuugaatsiaq, western Greenland. *Nat. Hazards Earth Syst. Sci.* <https://doi.org/10.5194/nhess-20-2521-2020> (2020).

20. Kutzner, D. Environmental change, resilience, and adaptation in nature-based tourism: conceptualizing the social-ecological resilience of birdwatching tour operations. *J. Sustain. Tourism* **27**, 1142–1166 (2019).
21. Macayeal, D. R., Abbot, D. S. & Sergienko, O. V. Iceberg-capsized tsunamigenesis. *Ann. Glaciol.* **52**, 51–56 (2011).
22. Black, T. & Kurtz, D. Maritime glacier retreat and terminus area change in Kenai Fjords National Park, Alaska, between 1984 and 2021. *J. Glaciol.* **69**, 251–265 (2023).
23. Bendixen, M. et al. Promises and perils of sand exploitation in Greenland. *Nat. Sustain.* **2**, 98–104 (2019).
24. Kochtitzky, W. & Copland, L. Retreat of Northern Hemisphere marine-terminating glaciers, 2000–2020. *Geophys. Res. Lett.* **49**, e2021GL096501 (2022).
25. *Operational Navigation Chart 1:1,000,000. Greenland (Denmark); Svalbard (Norway) Sheet A-1*, Edition 1 (US Aeronautical Chart and Information Center, 1969).
26. *Operational Navigation Chart 1:1,000,000. Greenland (Denmark) Sheet B-9*, Edition 1 (US Defense Mapping Agency Aerospace Center, 1968).
27. Harrison, J. C. et al. *Geological Map of the Arctic, 'A' Series Map, 2159A* (Natural Resources Canada, 2011).
28. Swift, D. A., Persano, C., Stuart, F. M., Gallagher, K. & Whitham, A. A reassessment of the role of ice sheet glaciation in the long-term evolution of the East Greenland fjord region. *Geomorphology* **97**, 109–125 (2008).
29. Bernard, M., Steer, P., Gallagher, K. & Egholm, D. L. The impact of lithology on fjord morphology. *Geophys. Res. Lett.* **48**, e2021GL093101 (2021).
30. Romanovsky, V. E., Smith, S. L. & Christiansen, H. H. Permafrost thermal state in the polar northern hemisphere during the international polar year 2007–2009: a synthesis. *Permafr. Periglac. Process* **21**, 106–116 (2010).
31. Hales, T. C. & Roering, J. J. Climatic controls on frost cracking and implications for the evolution of bedrock landscapes. *J. Geophys. Res. Earth Surf.* <https://doi.org/10.1029/2006JF000616> (2007).
32. Ochwat, N., Scambos, T., Fahnestock, M. & Stammerjohn, S. Characteristics, recent evolution, and ongoing retreat of Hunt Fjord Ice Shelf, northern Greenland. *J. Glaciol.* **69**, 57–70 (2023).
33. White, A. & Copland, L. Loss of floating glacier tongues from the Yelverton Bay region, Ellesmere Island, Canada. *J. Glaciol.* **65**, 376–394 (2019).
34. White, A. & Copland, L. Area change of glaciers across Northern Ellesmere Island, Nunavut, between ~1999 and ~2015. *J. Glaciol.* **64**, 609–623 (2018).
35. Benn, D. I., Warren, C. R. & Mottram, R. H. Calving processes and the dynamics of calving glaciers. *Earth Sci. Rev.* **82**, 143–179 (2007).
36. Cook, S. J. & Swift, D. A. Subglacial basins: their origin and importance in glacial systems and landscapes. *Earth Sci. Rev.* **115**, 332–372 (2012).
37. McNabb, R. W. & Hock, R. Alaska tidewater glacier terminus positions, 1948–2012. *J. Geophys. Res. Earth Surf.* **119**, 153–167 (2014).
38. Slater, D. A. et al. Estimating Greenland tidewater glacier retreat driven by submarine melting. *Cryosphere* **13**, 2489–2509 (2019).
39. Straneo, F. & Heimbach, P. North Atlantic warming and the retreat of Greenland's outlet glaciers. *Nature* **504**, 36–43 (2013).
40. Cowton, T. R., Sole, A. J., Nienow, P. W., Slater, D. A. & Christoffersen, P. Linear response of east Greenland's tidewater glaciers to ocean/atmosphere warming. *Proc. Natl Acad. Sci. USA* **115**, 7907–7912 (2018).
41. Carr, J. R., Stokes, C. R. & Vieli, A. Threefold increase in marine-terminating outlet glacier retreat rates across the Atlantic Arctic: 1992–2010. *Ann. Glaciol.* **58**, 72–91 (2017).
42. Mattingly, K. S. et al. Increasing extreme melt in northeast Greenland linked to foehn winds and atmospheric rivers. *Nat. Commun.* **14**, 1743 (2023).
43. Haacker, J., Wouters, B., Fettweis, X., Glissenaar, I. A. & Box, J. E. Atmospheric-river-induced foehn events drain glaciers on Novaya Zemlya. *Nat. Commun.* **15**, 7021 (2024).
44. Bjørk, A. A. et al. An aerial view of 80 years of climate-related glacier fluctuations in southeast Greenland. *Nat. Geosci.* **5**, 427–432 (2012).
45. Cook, A. J. et al. Atmospheric forcing of rapid marine-terminating glacier retreat in the Canadian Arctic Archipelago. *Sci. Adv.* **5**, eaau8507 (2019).
46. Ali, A. et al. Glacier area changes in Novaya Zemlya from 1986–89 to 2019–21 using object-based image analysis in Google Earth Engine. *J. Glaciol.* **69**, 1305–1316 (2023).
47. Sund, M., Lauknes, T. R. & Eiken, T. Surge dynamics in the nathorstbreen glacier system, Svalbard. *Cryosphere* **8**, 623–638 (2014).
48. Koppes, M. et al. Observed latitudinal variations in erosion as a function of glacier dynamics. *Nature* **526**, 100–103 (2015).
49. Cook, S. J., Swift, D. A., Kirkbride, M. P., Knight, P. G. & Waller, R. I. The empirical basis for modelling glacial erosion rates. *Nat. Commun.* **11**, 759 (2020).
50. Herman, F., De Doncker, F., Delaney, I., Prasicek, G. & Koppes, M. The impact of glaciers on mountain erosion. *Nat. Rev. Earth Environ.* **2**, 422–435 (2021).
51. Patton, H. et al. The extreme yet transient nature of glacial erosion. *Nat Commun* **13**, 7377 (2022).
52. Larsen, C. F., Motyka, R. J., Freymueller, J. T., Echelmeyer, K. A. & Ivins, E. R. Rapid uplift of southern Alaska caused by recent ice loss. *Geophys. J. Int.* **158**, 1118–1133 (2004).
53. Jiang, Y., Dixon, T. H. & Wdowinski, S. Accelerating uplift in the North Atlantic region as an indicator of ice loss. *Nat. Geosci.* **3**, 404–407 (2010).
54. Kavan, J. & Szczypińska, M. New and lost coast due to retreat/advance of Northern Hemisphere marine-terminating glaciers in the twenty-first century. *Zenodo* <https://doi.org/10.5281/zenodo.14538245> (2024).
55. Murray, T. et al. Extensive retreat of Greenland tidewater glaciers, 2000–2010. *Arct. Antarct. Alp. Res.* **47**, 427–447 (2015).
56. Dowdeswell, J. A. in *Arctic Ice Shelves and Ice Islands* (eds Copland, L. et al.) 55–74 (Springer Nature, 2017).
57. Wegmann, M., Gudmundsson, G. H. & Haeberli, W. Permafrost changes in rock walls and the retreat of alpine glaciers: a thermal modelling approach. *Permafr. Periglac. Process* **9**, 23–33 (1998).
58. Reinson, G. E. & Rosen, P. S. Preservation of ice-formed features in a subarctic sandy beach sequence: geologic implications. *J. Sediment. Res.* **52**, 463–471 (1982).
59. Lim, M. et al. Arctic rock coast responses under a changing climate. *Remote Sens. Environ.* **236**, 111500 (2020).
60. Mamot, P., Weber, S., Schröder, T. & Krautblatter, M. A temperature- and stress-controlled failure criterion for ice-filled permafrost rock joints. *Cryosphere* **12**, 3333–3353 (2018).
61. Luetzenburg, G. et al. Sedimentary coastal cliff erosion in Greenland. *J. Geophys. Res. Earth Surf.* **128**, e2022JF007026 (2023).
62. Nehyba, S., Hanáček, M., Engel, Z. & Stachoň, Z. Rise and fall of a small ice-dammed lake—role of deglaciation processes and morphology. *Geomorphology* **295**, 662–679 (2017).
63. Bendixen, M. et al. Delta progradation in Greenland driven by increasing glacial mass loss. *Nature* **550**, 101–104 (2017).
64. Higman, B. et al. The 2015 landslide and tsunami in Taan Fiord, Alaska. *Sci. Rep.* **8**, 12993 (2018).

65. Obu, J. et al. Northern Hemisphere permafrost map based on TTOP modelling for 2000–2016 at 1km² scale. *Earth Sci. Rev.* **193**, 299–316 (2019).
66. Hersbach, H. et al. *ERA5 Monthly Averaged Data on Single Levels From 1940 to Present* (C3S CDS, accessed 28 August 2024).

Publisher's note Springer Nature remains neutral with regard to jurisdictional claims in published maps and institutional affiliations.

Open Access This article is licensed under a Creative Commons Attribution 4.0 International License, which permits use, sharing, adaptation, distribution and reproduction in any medium or format,

as long as you give appropriate credit to the original author(s) and the source, provide a link to the Creative Commons licence, and indicate if changes were made. The images or other third party material in this article are included in the article's Creative Commons licence, unless indicated otherwise in a credit line to the material. If material is not included in the article's Creative Commons licence and your intended use is not permitted by statutory regulation or exceeds the permitted use, you will need to obtain permission directly from the copyright holder. To view a copy of this licence, visit <http://creativecommons.org/licenses/by/4.0/>.

© The Author(s) 2025

Methods

Remote sensing data

We used the dataset of Northern Hemisphere marine-terminating glaciers retreat between 2000 and 2020²⁴ to identify all marine-terminating glaciers in the Northern Hemisphere. We manually digitized the new coastline that was exposed as a result of glacier retreat using satellite imagery. Similarly, we also digitized the coastline that disappeared as a result of glacier advances. We mapped the vector shapefiles of the above-mentioned dataset using 2020 Sentinel-2 (cloud-free, false colour—bands 8,4,3 in 10-m resolution) optical imagery to delimit new shoreline and cross-check glacier margin accuracy. We checked glacier advance and coastline loss using Landsat-7 cloud-free, true colour imagery from 2000 (30-m resolution). For a few areas where the Sentinel-2 images were not available (the northernmost parts of Canada and Greenland) we used Sentinel-1 (20 m × 40 m) or Sentinel-3 OLCI (300 m) images.

We followed ref. 24 and used the Randolph Glacier Inventory v.6 (ref. 67) to provide a unique identifier for each glacier. The shapefiles of the newly emerged coastline and the coastline lost including the basic derived parameters in the attribute tables are provided.

Environmental factors of the new coastlines

To provide a general characterization of new coastline, digitized lines were split using the ‘Split lines by maximal length’ algorithm in QGIS with maximum line length set to 500 m. Each of the resulting 6,699 coastline segments was then supplemented with an attribute of rock type, permafrost zone, precipitation and temperature. The geological description is generalized to categories of sedimentary, igneous, metamorphic and undivided rocks based on the geological map of the Arctic²⁷. Bedrock is indicated as metamorphic for medium or high grade of metamorphism. The work of ref. 27 does not cover the southern part of Alaska (below 60° N), so the missing sites were filled using a geologic map of Alaska⁶⁸. Permafrost classification follows ref. 65. If a segment is covered by ice according to the geological or permafrost map the nearest rock/permafrost category is attributed. When two or more geological/permafrost classes are present along coastline segment the class with the longest overlap is chosen.

The supporting climatic indices (air temperature and precipitation) were derived from the gridded monthly averages of the ERA5 reanalysis provided by the ECMWF (<https://cds.climate.copernicus.eu/datasets>). Monthly averaged values north of 50° N were downloaded for the period 2000–2020. The single average value was then attributed to each line segment of the new coast shapefile. The values presented in figures are in degrees centigrade at 2 m above the surface for air temperature and total annual precipitation amount (summed rainfall and snowfall) in millimetres per year.

We used ITS_LIVE glacier velocity data, which were extracted near the termini of each glacier⁴, as a proxy for glacier erosion potential.

Cartographic projection and validation of results

Retreat areas for individual glaciers from period 2000–2020, used for calculating NC–RA ratio for regions and for individual glaciers, were taken from ref. 24. NC–RA ratio was calculated for individual glaciers by dividing length of new coastline (in kilometres) by corresponding retreat area (in kilometres squared). Digitizing of the coastline and calculation of the coastline length were undertaken in QGIS 3.22; final versions of the maps were produced in QGIS 3.34. We projected each line into a unique orthographic projection suitable for that location to calculate the length of the feature to eliminate the impact of area distortion²⁴. The graphical outputs are projected in the WGS84 Arctic Polar Stereographic projection (EPSG 3995). We used late summer images (preferably August/September or July if other images were not available) to avoid any snow cover which can make it difficult to distinguish between snow cover on land and the glacier surface. We checked visually for the presence of an ice-cored lateral moraine on the edge of the glacier, which is often visible, and excluded it from the

newly identified coastline. In the process of delimitation of new coasts, we also identified new islands and made an inventory of islands larger than 0.5 km² that appeared between 2000 and 2020. New islands found were then compared to the previous studies^{12,13}.

Uncertainties

The uncertainty is based on the spatial resolution of the satellite images used for the coastline delimitation. Each line segment of the digitized coastline was thus considered to have a 10-m uncertainty on each side. A similar uncertainty would apply to the positional accuracy of the digitized coastline; however, this does not affect the calculated length. Each line side is treated as an independent error source, so the total uncertainty is calculated as a root of summed squared values (following, for example, ref. 24)—giving the equation $un = \frac{\sqrt{l}}{100}$, where l is the number of coastline segments and the unit is kilometres.

However, the scale at which imagery is digitized does affect the length, but only in comparison to lengths at differing scales²⁴. On the basis of imagery resolution we digitized the coastline at a scale of 1:5,000. Thus, our lengths are internally consistent, but may differ from those of other studies at different scales.

Data availability

Data are available as follows: (1) polygons showing marine-terminating glaciers retreat/advance between 2000 and 2020 are available from the polar data catalogue (http://www.polardata.ca/pdcsearch/PDCSearch-DOI.jsp?doi_id=13257) and (2) all the satellite imagery data used in this study can be freely downloaded from SentinelHub EO browser (<https://apps.sentinel-hub.com/eo-browser>). The generated datasets of (1) new and lost coastline segments, (2) new and lost coastline grouped by individual glaciers and (3) fragments of new coastline segments with general geological, permafrost zone and climatic characteristics, are available via Zenodo at <https://doi.org/10.5281/zenodo.14538245> (ref. 54). Correspondence and requests for materials should be addressed to M.S. (malgorzata.szczybinska2@uwr.edu.pl) and J.K. (jkavan@prf.jcu.cz).

References

67. RGI Consortium. Randolph Glacier Inventory—A Dataset of Global Glacier Outlines, Version 6. NSIDC <https://doi.org/10.7265/4m1f-gd79> (2017).
68. Wilson, F. H., Hults, C. P., Mull, C. G. & Karl, S. M. *Geologic Map of Alaska* (USGS, 2015); <https://doi.org/10.3133/sim3340>

Acknowledgements

This study is the contribution to the National Science Centre project ‘GLAVE Paraglacial coasts transformed by tsunami waves—past, present and warmer future’ (UMO2020/38/E/ST10/00042) awarded to M.C.S. L.F. was supported by the NSF Award (number: 1927553) ‘Collaborative Research: AccelNet: Permafrost Coastal Systems Network (PerCS-Net)—A Circumpolar Alliance for Arctic Coastal Community Information Exchange’. Open access fee has been generously covered by the University of Wrocław—decision BPIDUB.4610.21.2025.KG—The Excellence Initiative—Research University.

Author contributions

J.K., M.C.S. and M.S. conceived the study idea. W.K. contributed to glaciological aspects of the study, while L.F. strengthened the sections on permafrost and M.B. worked on the broader significance for the study of coastal change and its inhabitants. M.S. and J.K. performed the data analyses. All co-authors contributed to analysing the results and deriving conclusions. J.K., M.S. and M.C.S. wrote the manuscript, with contributions from all co-authors.

Competing interests

The authors declare no competing interests.

Additional information

Supplementary information The online version contains supplementary material available at <https://doi.org/10.1038/s41558-025-02282-5>.

Correspondence and requests for materials should be addressed to Jan Kavan or Małgorzata Szczypińska.

Peer review information *Nature Climate Change* thanks Simon Cook, Martin Jakobsson and Nicholas Midgley for their contribution to the peer review of this work.

Reprints and permissions information is available at www.nature.com/reprints.